

Design of a flexure for surface forces apparatus

D. Devaprakasam and S. K. Biswas

Citation: [Review of Scientific Instruments](#) **74**, 1228 (2003); doi: 10.1063/1.1533792

View online: <http://dx.doi.org/10.1063/1.1533792>

View Table of Contents: <http://scitation.aip.org/content/aip/journal/rsi/74/3?ver=pdfcov>

Published by the [AIP Publishing](#)

Articles you may be interested in

[Modeling, design, and analysis of interferometric cantilevers for time-resolved force measurements in tapping-mode atomic force microscopy](#)

J. Appl. Phys. **109**, 064316 (2011); 10.1063/1.3553852

[Evading surface and detector frequency noise in harmonic oscillator measurements of force gradients](#)

Appl. Phys. Lett. **97**, 044105 (2010); 10.1063/1.3465906

[Design and performance of a high-resolution frictional force microscope with quantitative three-dimensional force sensitivity](#)

Rev. Sci. Instrum. **76**, 043704 (2005); 10.1063/1.1889233

[Surface-force measurement with a laser-trapped microprobe in solution](#)

Appl. Phys. Lett. **80**, 3448 (2002); 10.1063/1.1468267

[Calibration of piezoelectric bimorphs for experiments in a surface forces apparatus](#)

Rev. Sci. Instrum. **71**, 3955 (2000); 10.1063/1.1288233



JANIS Does your research require low temperatures? Contact Janis today.
Our engineers will assist you in choosing the best system for your application.

10 mK to 800 K LHe/LN₂ Cryostats
Cryocoolers Magnet Systems
Dilution Refrigerator Systems
Micro-manipulated Probe Stations

sales@janis.com www.janis.com
Click to view our product web page.

Design of a flexure for surface forces apparatus

D. Devaprakasam and S. K. Biswas^{a)}

Department of Mechanical Engineering, Indian Institute of Science, Bangalore 560 012, India

(Received 8 May 2001; accepted 22 October 2002)

We report the design of a variation of a double cantilever flexure system used for the measurement of displacement and force in surface force apparatus (SFA). The new force sensor is called dual double cantilever. The simple cantilever flexure suffers rotation, sideways deflection, and thermal expansion at the free end when loaded normally and asymmetrically. In the double cantilever these errors are minimized to a second order. In the dual double cantilever flexure the stiffness is enhanced 16 times as that of a single cantilever flexure but the rotation, sideways deflection, and thermal expansion at the free end are brought to many orders below the instrument resolutions. The new design enables the measurement of deflection by optical and capacitive sensing methods. The stiffness and the strain of the aluminum alloy [AUG1(2024)] flexure were estimated [dimensions, length ($l=50.5$ mm), breadth ($b=10.5$ mm), and thickness ($t=1.2$ mm)] by finite element method and were also validated experimentally. The finite element method was also used to create a map for the selection of a flexure geometry relevant to the properties of material under investigation by a SFA or a nanoindenter. © 2003 American Institute of Physics. [DOI: 10.1063/1.1533792]

I. INTRODUCTION

Normal load bearing and shear properties of liquids in confined volumes are important engineering design parameters. Measurement of mechanical properties thus needs sensors which have high sensitivity. When the order of forces are very small as in the case of atomic force microscopy (AFM), a highly compliant sensor is useful.¹ However, when the order of forces are high (ranging from μN to 100 mN) as in the case of surface force apparatus (SFA),^{2,3} geometric distortion of the compliant sensor gives rise to nonlinear responses and may indeed lead to erroneous results. Here we address the design of a cantilever based sensor system for a SFA which we intend to use to measure nanotribological properties such as contact stiffness, adhesion, viscoelasticity, and molecular wear resistance under extreme conditions of temperature and pressure. SFA is used to measure van der Waal's forces between surfaces of well defined geometry. Tabor and Winterton,⁴ Israelachvili⁵ used a single cantilever as a force sensor in their SFA to measure the Hamaker constant, jump distance D_j , and adhesion. In a further development of SFA, Israelachvili² used a double cantilever force sensor to measure van der Waal's, electrostatic, colloidal, hydrophobic, hydrophilic, solvation, and structural forces operating in millimeter to nanometer range. Recent SFA developments enable the measurement of properties of polymeric monolayers and complex molecular systems.^{2,3,6}

II. REQUIREMENT OF SENSOR

The primary requirement is that the out-of-plane rotation of the specimen platform under a normal load should be well below the resolution of the measuring instrument (taken here to be 10^{-9} m). This constraint ensures the normality of the

vertical displacement of the indenter with respect to the horizontal top plane of the specimen and eliminates the possibility of any resolved component of the normal force to act between the probe and the sample. This also aids in the optical measurement of the platform displacement in the reflective mode and allows the positioning of a capacitive sensor below the platform, if so required. The in-plane and the out-of-plane distortions under thermal loading should also be low. If there is an out-of-plane thermally induced distortion it should be uniform over the entire area of the platform. To ensure high signal-to-noise ratio the natural frequency of the system should be much higher than that of the operating frequency. Under the severest loading, the load-displacement characteristics of the cantilever should retain its linearity disallowing any yield in the flexure body. The disadvantages of using a single cantilever as a force or displacement sensor in applications such as SFA is that it suffers free end rotations and significant dimensional changes under thermal loading. The latter are sources of first order errors in measurement. The free end rotation is largely prevented by rigidly joining two parallel single cantilevers by an elastic ligand. When a vertical load is applied at the free end, the ligand ensures that there is only vertical deflection by providing counter moments (see the Appendix for details) to the two cantilever members at the connected joints. Now if this ligand which lies in a vertical plane is the upright part of an L plate, the horizontal part can be used to support a specimen to be tested in an apparatus such as SFA. The advantage gained by this arrangement is of course at the cost of the flexure sensitivity. The thickness of the two parallel plates adds to the stiffness. The stiffness of the double cantilever increases 8 times as that of the single cantilever, this is clearly observed from the relation [stiffness $K=2Ebt^3/(l^3)$ where E is the Young's modulus, b the width, t the thickness, and l the length of the cantilever]. Though the free end rotation is reduced in this

^{a)}Electronic mail: skbis@mecheng.iisc.ernet.in

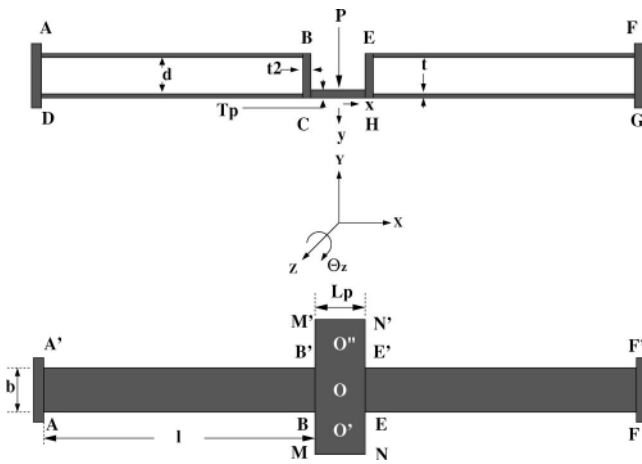


FIG. 1. Dual double cantilever, L-length (50.5 mm), (b) breadth (10.5 mm), (t) thickness (1.2 mm), (t2) thickness of vertical member (2.4 mm), (L_p) length of platform (12 mm), (T_p) thickness of the platform (3 mm), x and y distortion due to heating: (a) elevation, (b) plan view.

arrangement, our FEM calculations show that it persists at the second order (10^{-2} times that of single cantilever) level.

We reduced this error to a level (10^{-9} times that of the single cantilever) less than the measurement resolution by configuring two identical double cantilever systems as connected parallel springs. This raises the overall stiffness to two times the single double cantilever system. We designate this new arrangement as dual double cantilever. We show that in this system the distortion due to thermal loading is also significantly reduced when compared to that of a single double cantilever system. A horizontal plate now connects the vertical ligands of the two double cantilever systems and the plate has no other freedom of movement except strictly in the vertical direction. The direction of loading is vertical but the arrangement can also take in-plane (horizontal) shear without distortion. In this new configuration, the horizontal platform can serve as a holder for a test sample, a guide for vertical movement, and act as a reflector or holder for a capacitor plate for displacement measurement.

We have used FEM analysis for the design of a dual double cantilever flexure. Experimental verification of the design and flexure performance being difficult *in situ*, i.e., once the flexure is incorporated into the final SFA configuration, we have fabricated a scaled up version of the flexure from a monoblock using wire cut (EDM) technique (the final SFA configuration would be fabricated in a similar manner) and tested our design code by measuring deflection and distortion under normal load. We report here the design and its experimental verification. We are aware of the potential of such a flexure system for displacement and/or force measurement in other microprobes such as a nanoindenter. We present a map, which at a glance gives the range of allowed dimensional ratios of the present configuration, and the limits of corresponding probe loads for groups of materials varying from short chain liquid polymers to ceramics.

III. DUAL DOUBLE CANTILEVER

Figure 1 shows the dual double cantilever beam. It consists of two pairs of single cantilevers (AB, CD and EF, GH)

connected at the free ends by rigid members BC and EH. The latter are connected by another rigid member CH on which the load is applied. The dual double cantilever configuration is an indeterminate structure. To obtain close form solution, the configuration is approximated to two parallel double cantilevers connected at the free end. The applied load P is shared equally between the two double cantilevers as $P/2$ and $P/2$. Using the symmetry of the dual double cantilever about the loading plane, a near close form solution could be arrived at by using the strain energy method. To a first order approximation the stiffness of the dual cantilever by this method (see the Appendix for details) is given by

$$K = \frac{4Ebt^3}{l^3}. \tag{1}$$

IV. FEM

The dual double cantilever flexure is modeled and analyzed statically and dynamically using the NASTRAN⁷ FEM software. The mesh consisted of four noded QUAD4 shell elements. The flexure material is assumed to be isotropic and linear elastic. The mesh size is refined and optimized. Figure 2(a) shows a FEM estimate of the vertical displacement of the dual double cantilever under a concentrated vertical load of 2N. It is of interest to us that the vertical displacements of the platform, ligands, and nonfixed end of the cantilever beam are the same, this ensures that the platform translates down vertically without warp, rotation, and twist. Figure 2(b) shows the horizontal (x) strain in the main cantilever body. The strain in the ligand and platform are low. Figure 2(c) shows the displacements of the dual double cantilever when the horizontal platform is heated to 200 °C by a massless heater placed on it. The figure shows that due to the expansion of the cantilever, the ligands rotate (θ_z) but the horizontal platform displaces vertically down without any distortion and rotation.

V. EXPERIMENTAL AND FEM VALIDATIONS

A dual double cantilever flexure carrying a loading platform C'D'DC (Fig. 1) was electrodischarge machined out of a rectangular monoblock of the aluminum alloy AU4G1(2024), heat treated to T4 condition. This monoblock material was chosen because of its low density and appropriate damping and hysteresis properties. The dimensions of the flexure arrived at using the FEM by considering the SFA constraints, are shown in Fig. 1. The end supports AD and FG are part of the vertical walls of the monoblock. The properties of the aluminum alloy AU4G1(2024) are: Young's modulus $E=72$ GPa; tensile strength 450–480 MPa; yield strength 290–340 MPa. Dead weights were put on a pan vertically suspended from O. A linear variable differential transformer (LVDT) was fixed to the top horizontal beam of the monoblock with its measuring tip touching the flexure at O' or O'' . Two strain gauges were pasted in the maximum horizontal (x) strain regions of the flexure, identified by the FEM analysis. The strains were measured with a resolution

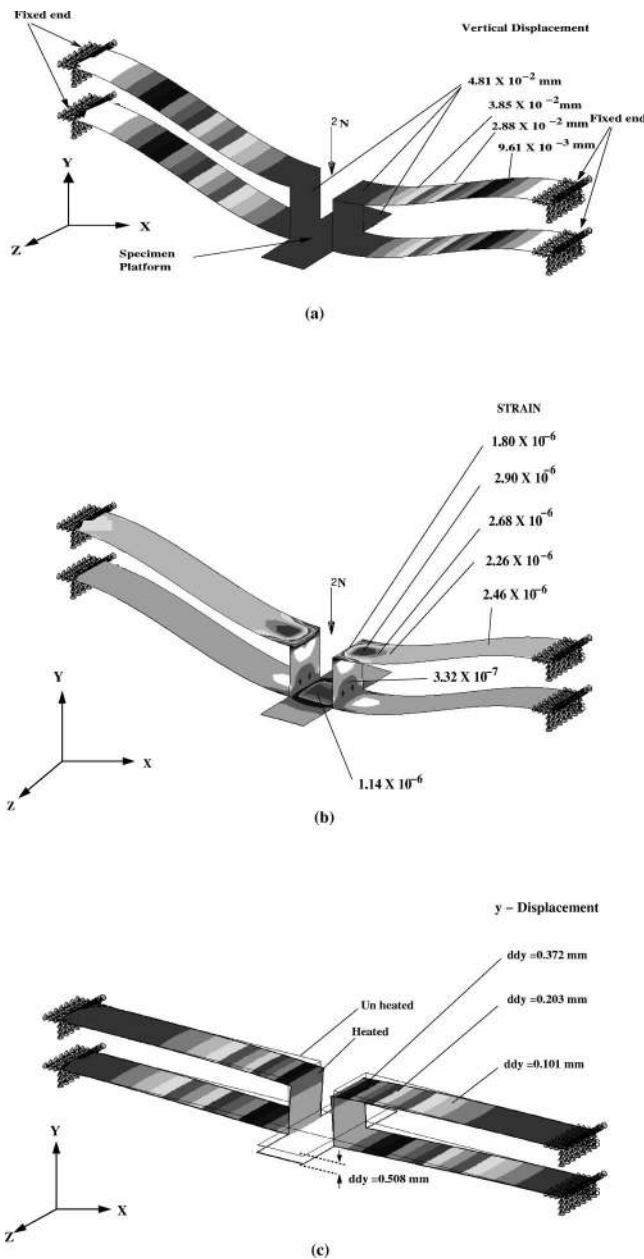


FIG. 2. (a) Vertical displacement of the dual double cantilever flexure due to a concentrated vertical load of 2N at the center of the specimen platform. The displacements scale with load. For example for a 2×10^{-6} N load the platform displacement is 4.49×10^{-8} mm (see Fig. 1 for flexure dimensions). (b) Horizontal (\times) strain in the dual double cantilever flexure due to a concentrated load of 2N at the center point of the specimen platform. (c) Vertical displacement of the dual double cantilever flexure due to steady state heating of the platform up to 200°C. ddy is the uniform vertical deflection of the platform.

of 1 microstrain. The flexure was designed for a load range of 10 mN–10 N, with the stiffness of the flexure being 4×10^4 N/m.

Figure 3 shows that the experimental load–displacement relation is linear and the FEM prediction follows this trend closely. The experimental strain–displacement relationship was also found to be linear and close to the FEM result.

Figure 4 shows the estimated θ_z (FEM) for single, double, and dual double cantilever flexures. θ_z increases with force for the single and the double cantilever flexures. For

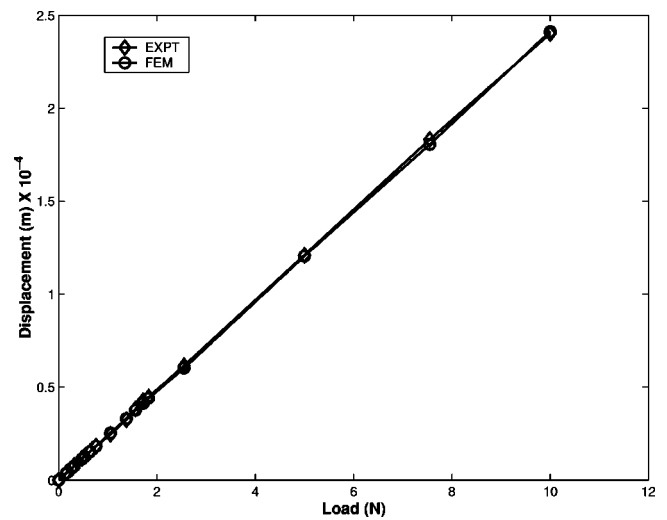


FIG. 3. Vertical displacement at the center point of the specimen platform vs displacement.

the dual double cantilever (Figs. 1 and 4) no rotation or distortion of the platen could be observed even at 10^{-2} N concentrated load. FEM estimates of x and y displacement under heated condition (up to 200 °C) showed substantial displacements of the cantilever edges for single and double cantilever systems. For the dual double cantilever the dimension of the loading platform in the x direction remains unchanged.

VI. DIMENSION SELECTION

Figure 5 gives the estimated (FEM) map for the selection of thickness to length ratio of the dual double cantilever. The cantilever stiffness is directly proportional to $(t/l)^3$ and the breadth “ b .” The stiffness is estimated here for $b=10.5$ mm. For monoblock fabrication this is a convenient dimension. For any other value of b the map may be simply scaled. Line L_A gives the limiting load at which the maximum shear stress in the cantilever is half the yield shear strength, at yield the maximum shear stress is equal to the yield shear

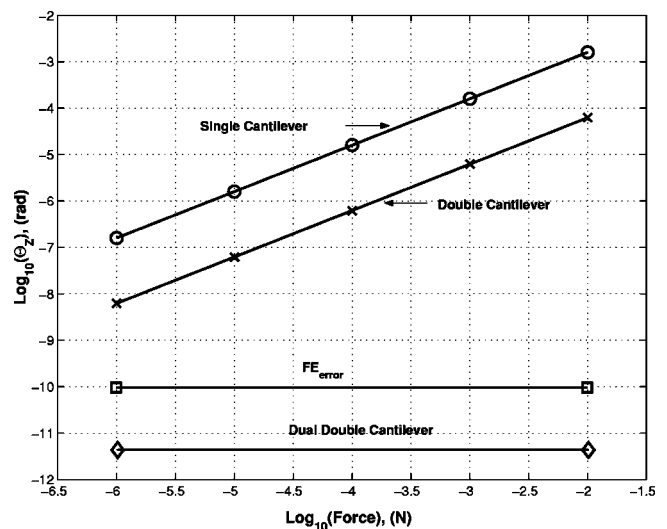


FIG. 4. Normal force vs θ_z (specimen platform) calibration graph, FE_{error} —finite element results show negligible θ_z .

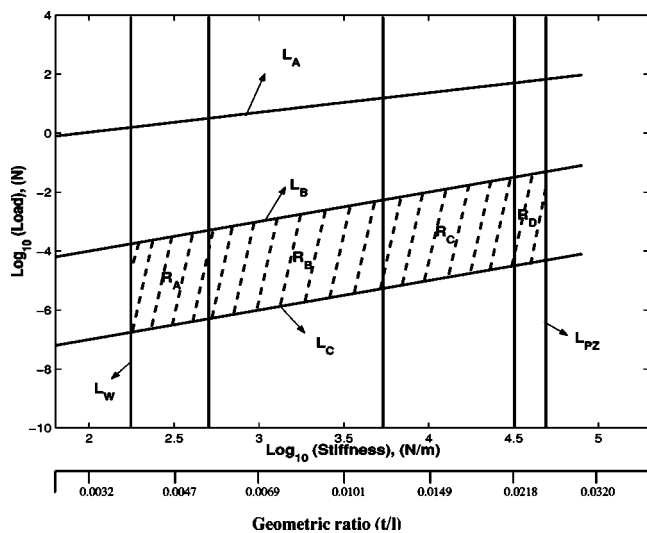


FIG. 5. Operational regimes map for dimensional selection of dual double cantilever flexure. R_A : rigid molecule, R_B : polymer, R_C : metal, R_D : ceramic, L_A : failure limit, L_W : frequency limit, L_C : sensor resolution, L_B : sensor range limit, L_{PZ} : driver stiffness limit. Breadth $b=10.5$ mm.

strength. Line L_W denotes the stiffness, at values less than the natural frequency of the system, $\omega_n < 200$ Hz (the maximum operating frequency is 10 Hz and it should be less than the natural frequency of the flexure system). Line L_{PZ} denotes the stiffness of the piezoelectric driver (for the SFA). Taking the displacement resolution of the system to be 1 nm, line L_C denotes the load, below which for a given stiffness the deflection is less than 1 nm. Line L_B denotes the load upper bound, at loads above which the upper displacement limit (assumed to be 1 mm) of the sensor (LVDT or photodiode) is exceeded. The operating region is bounded by lines L_B , L_C , L_W , and L_{PZ} . We now take different generic material types and estimate contact stiffness for the weakest and strongest material of a type for an indentation depth of 10 nm. The contact stiffness is given by

$$S = 2E^*a, \quad (2)$$

where a is the contact radius calculated using Hertzian equations and E^* is the reduced modulus. For soft materials such as rigid molecules octamethylcyclotetrasiloxane (OMCTS) ($E \approx 1-100$ MPa) and elastomers ($E \approx 100-1000$ MPa) the contact stiffnesses are calculated for 500 μm diameter indenter executing an indentation depth of 10 nm. For polymers ($E \approx 1-50$ GPa), metals ($E \approx 50-250$ GPa), and ceramics ($E \approx 250-400$ GPa) the contact stiffnesses calculated for a 500 nm diameter tip and depth of indentation of 10 nm. Obtaining S_{\min} and S_{\max} for a material type, we assume that the desired flexure stiffness should be in the $S_{\min}-S_{\max}$ range to avoid contact instability.

Given a material type, Fig. 5 may now be used to select a possible range of (t/l) ratio and the lower and upper bounds of the operating load. For example, for a long chain (solid) polymer being indented, the range of (t/l) is $\sim 0.005-0.0120$ and the permissible load range is approximately $1 \mu\text{N}-1$ mN.

VII. DISCUSSION

Cantilever springs have been used to measure forces between surfaces in vapor³ and liquid medium² as well as to measure mechanical properties of liquids^{6,8} confined between surfaces. In the surface force apparatus the gap between two transparent mica surfaces are measured directly using multiple beam interferometry. For measuring mechanical properties of liquid trapped between opaque solids of engineering interest indirect measurement of the gap is made.³ Vertical displacements of the two plates connected to two double cantilever systems, one carrying the indenter and the other the sample are measured by capacitors. The difference between the two displacements gives the change in the gap or the specimen deformation. These cantilevers, in principle, ensure vertical translation in response to vertical (normal) loading. The advantage of this system is that as the change in the gap is estimated on a “differential principle,” errors associated with absolute measurements are minimized.

We have shown that on normal loading the edges of the double cantilever springs undergo rotation, strict vertical displacement is not ensured on normal loading. Furthermore, if the equipment is displacement controlled, the two cantilever systems are acted upon by different normal forces and undergo different degrees of rotation. This introduces error in the normality of loading. The arrangement runs into further difficulties if the sample is heated *in situ*. The double cantilever edges undergo unconstrained expansion on heating introducing uncertainty in sample location and unwanted stressing of the sample if the sample is clamped to the double cantilever edge.

If two sets of the dual double cantilever beams are placed parallel and coaxial to each other such that the indenter is mounted on one and the sample on the other, the present results show that vertical actuation of the indenter would ensure a strict vertical translation of the sample. If such an arrangement is now considered as the heart of an instrument for measurement of surface forces or mechanical properties of constrained medium the arrangement can be seen to take advantage of the principle of differential displacement while being unencumbered by the limitations of the previous systems in relation to *in situ* sample heating and normality of loading. In doing this, one of course, sacrifices resolution as each dual double cantilever system is twice as stiff as a double cantilever system. This may not be a severe handicap as strict guarantee of normality of loading under all conditions (within the limits of yield) allows certain relaxation of the stiffness requirement to boost resolution. One disadvantage of the double cantilever system is that its use is limited to probing relatively soft samples. In probing stiff samples as in nanoindentation the orders of forces are high and the rotation of the sample holder [Eq. (9), Appendix] may become a prohibitive factor. As the rotation under any level of normal loading is nil when dual double cantilever systems are used for measurement, the latter system (with the use of design maps as given in Fig. 5) can be used for a wide variety of probing, from the measurement of surface forces in liquid environment to nanoindentation of solids.

A dual double cantilever flexure was designed and ex-

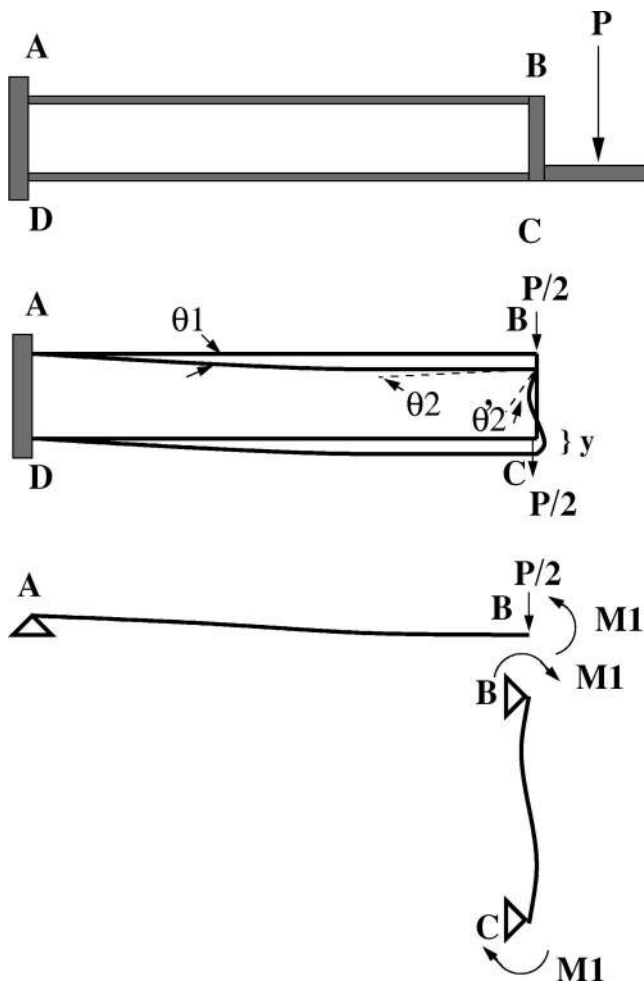


FIG. 6. Schematic diagram of double cantilever, giving the forces, moments, and deflections due to a concentrated load P .

perimentally tested for load displacement linearity. The cantilever configuration ensures strict vertical movement of the point of load application in response to vertical actuation, normality of loading is thus maintained. FEM simulations show that heating of the central ligand of the system does not generate any unwanted distortion of the ligand. The flexure system is suitable for incorporation with equipments used for a wide variety of probing, ranging from measurement of surface forces in liquid environment to nanoindentation of solids.

ACKNOWLEDGMENTS

The authors thank Defense Research Development Organization, Government of India, for providing a necessary grant for developing the SFA. We thank A. K. Patil for help with the electronics. We also thank H. S. Shamsunder for his laboratory support.

APPENDIX: DERIVATION OF STIFFNESS FOR THE DUAL DOUBLE CANTILEVER BY THE STRAIN ENERGY METHOD

Figure 1 shows the dual double cantilever beam. The double cantilever consists of two simple cantilevers of the same material and dimensions, they are separated by a dis-

tance d , and at the free ends they are connected by L-shaped rigid thin plate of the same material as that of the cantilevers (shown in Fig. 6). The end member ensures in-planar deflection in the y direction by providing counter moments to the two cantilever members at the connected joints. The portions AB and CD represent two cantilever members and the portion BC represents the vertical ligand connection at the free end.

Now, let P be the load applied at the free end. Since BC is more rigid when compared to the cantilever and the distance OC is very small compared to the span length of the cantilevers, we assume that the load P is equally shared between the two cantilever plates, i.e., $P/2$ at C and $P/2$ at B.

Consider a section mn at a distance x from B, then the angle θ_2 at B is given by Castigliano’s theorem⁹ as

$$\theta_2 = \frac{\partial U}{\partial M_1} \tag{A1}$$

$$= \frac{1}{EI_1} \int_0^l M \frac{\partial M}{\partial M_1} dx, \tag{A2}$$

where I_1 is the moment of inertia of portion AB and $M = P'x - M_1$ and $P' = P/2$. Substituting M in Eq. (A2) we get

$$\theta_2 = \frac{Pl^2}{4EI_1} - \frac{M_1 l}{EI_1}. \tag{A3}$$

Similarly, deflection of the portion AB is given by

$$y = \frac{1}{EI_1} \int_0^l (-M_1 + Px)x dx, \tag{A4}$$

$$= \frac{1}{EI_1} \left(-\frac{M_1 l^2}{2} + \frac{Pl^3}{6} \right). \tag{A5}$$

Consider the portion BC which is simply supported with moment M_1 acting at both ends, in the same direction. R_1 is the reaction at end B, and considering the total moment acting at B,

$$R_1 d = 2M_1.$$

The total moment acting at the end B of portion BC is

$$M = \left(M_1 - \frac{2M_1}{d} x \right). \tag{A6}$$

From Castigliano’s theorem, θ'_2 is given by

$$\theta'_2 = \frac{M_1 d}{6EI_2}. \tag{A7}$$

Since the equilibrium condition at B requires

$$\theta_2 = \theta'_2, \tag{A8}$$

$$M_1 = \left\{ \frac{Pl}{4 \left(1 + \frac{dI_1}{6II_2} \right)} \right\}.$$

Substituting M_1 in Eq. (A5) we get

$$y = \frac{Pl^3}{2EI_1} \left\{ \left(\frac{1}{12} + \frac{dI_1}{18lI_2} \right) \right. \\ \left. \left(1 + \frac{dI_1}{6lI_2} \right) \right\}. \quad (\text{A9})$$

The stiffness K of the double cantilever is

$$K = \frac{P}{y} \quad (\text{A10})$$

$$= \frac{2EI_1}{l^3} \left\{ \left(1 + \frac{dI_1}{6lI_2} \right) \right. \\ \left. \left(\frac{1}{12} + \frac{dI_1}{18lI_2} \right) \right\}, \quad (\text{A11})$$

as $I_2 \gg I_1$ and $l \gg d$:

$$K = \frac{24EI_1}{l^3}, \quad (\text{A12})$$

$$= \frac{2Ebt^3}{l^3}. \quad (\text{A13})$$

The stiffness of the dual double cantilever is

$$K = \frac{4Ebt^3}{l^3}. \quad (\text{A14})$$

The stiffness of the dual double cantilever system is twice that of a double cantilever and 16 times that of a simple cantilever.

¹G. Binning, C. F. Quate, and Ch. Gerber, Phys. Rev. Lett. **56**, 930 (1986).

²J. N. Israelachvili and P. M. McGuiggan, J. Mater. Res. **5**, 2223 (1990).

³J. M. Georges, S. Millet, J. L. Loubet, and A. Tonck, J. Chem. Phys. **98**, 7345 (1993).

⁴D. Tabor and R. H. S. Winterton, Proc. R. Soc. London, Ser. A **312**, 435 (1969).

⁵J. N. Israelachvili and D. Tabor, Proc. R. Soc. London, Ser. A **331**, 19 (1972).

⁶J. Peachey, J. Van Alsten, and S. Granick, Rev. Sci. Instrum. **62**, 463 (1991).

⁷MSC.visual NASTRAN 2001, MSC Software Corp., Los Angeles, CA.

⁸S. C. Bae and S. Granick, Rev. Sci. Instrum. **71**, 3955 (2000).

⁹S. Timoshenko, *Strength of Materials*, 3rd Indian ed. (CBS, Delhi, 1998), Vols. 1 and 2.